

Chemical Science

Accepted Manuscript



This is an *Accepted Manuscript*, which has been through the Royal Society of Chemistry peer review process and has been accepted for publication.

Accepted Manuscripts are published online shortly after acceptance, before technical editing, formatting and proof reading. Using this free service, authors can make their results available to the community, in citable form, before we publish the edited article. We will replace this *Accepted Manuscript* with the edited and formatted *Advance Article* as soon as it is available.

You can find more information about *Accepted Manuscripts* in the [Information for Authors](#).

Please note that technical editing may introduce minor changes to the text and/or graphics, which may alter content. The journal's standard [Terms & Conditions](#) and the [Ethical guidelines](#) still apply. In no event shall the Royal Society of Chemistry be held responsible for any errors or omissions in this *Accepted Manuscript* or any consequences arising from the use of any information it contains.

EDGE ARTICLE

Metal–Organic Framework Encapsulated Pd Nanoparticles: towards Advanced Heterogeneous Catalysts

Cite this: DOI: 10.1039/x0xx00000x

Received 00th January 2012,
Accepted 00th January 2012

DOI: 10.1039/x0xx00000x

www.rsc.org/

Liyu Chen,^a Huirong Chen,^a Rafael Luque,^{b*} and Yingwei Li^{a*}

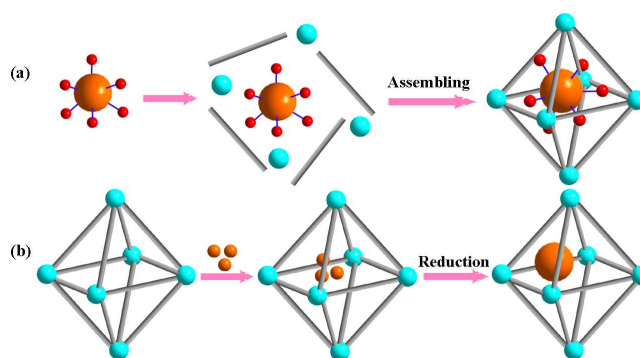
A novel synthesis strategy is developed to encapsulate palladium precursors through ligand design prior to MOF assembly, achieving uniformly distributed palladium NPs inside the cavities of MOFs. This strategy can avoid the different diffusion resistance between external and internal surfaces, and thus allow metal precursors to be easily deposited into the pores and evenly distributed within MOF networks. The embedded Pd NPs exhibited excellent shape-selectivity in olefin hydrogenation, as well as high catalytic efficiencies in aerobic oxidation of alcohols and reduction of nitrobenzene, showing significantly enhanced catalytic activity and stability as compared to those synthesized using a traditional impregnation method. The superior catalytic activity and stability came from the synergetic effects of nano-confinement and electron-donation offered by the MOF framework.

Introduction

Metal-nanoparticles (MNPs) have recently received a staggering degree of attention, due to their high chemical activities and specificities.¹ Due to their high surface area to volume ratio, the control of their size, shape, and dispersion is key to enhance the catalytic activity and selectivity of MNPs.² A promising approach to achieve this goal is to assemble MNPs inside porous materials (e.g. zeolites, mesoporous aluminosilicates, and other porous inorganic or organic materials) by efficiently limiting the growth of MNPs in the confined cavities.³ This has been rarely considered to date, with most methodologies dealing with a post-synthetic impregnation step for MNPs incorporation.⁴

Metal-organic frameworks (MOFs) emerged as a class of highly promising porous materials, owing to their superior properties including diverse chemical compositions, large surface areas and porosity as compared to related micro- and meso-porous materials.⁵ These properties make MOFs very appropriate candidates for the incorporation of active phases for catalytic applications (e.g. MNPs).⁶ In some cases, catalytically active MOFs are even designed without any need for further active phase incorporation in a range of catalytic applications.⁷ Additionally, MOFs constructed by metal nodes and aromatic linkers can certainly establish charge transfer interactions by coordination or π - π forces, offering an additional advantages for the stabilisation/activity improvement of MNPs as compared to other supports (e.g., zeolites, and mesoporous aluminosilicates).^{8,9} Aggregation and leaching issues generally taking place during catalytic reactions may be minimised in MOF-

encapsulated MNPs due to confinement and electronic effects offered by MOF networks. Advanced heterogeneous nanocatalysts can then be simply designed with significantly improved catalytic performances, similar to those already reported for room temperature catalytic processes.¹⁰



Scheme 1. Encapsulation of metal NPs within MOFs via: a) building MOF structures around pre-formed metal NPs, b) using MOFs as templates to generate NPs. Color coding: cyan, secondary building unit of MOFs; grey, organic linkers; orange, metal precursors or NPs; red, stabilizing agents.

MOFs with embedded metal/metal oxide NPs can be envisaged starting from a) building MOF structures around pre-formed NPs or b) using MOFs as templates to generate NPs (Scheme 1).¹¹ The former approach, reported very recently,¹² often requires certain surfactants, capping agents or even ions for the stabilization of pre-synthesized MNPs. However, such stabilizing agents are difficult to

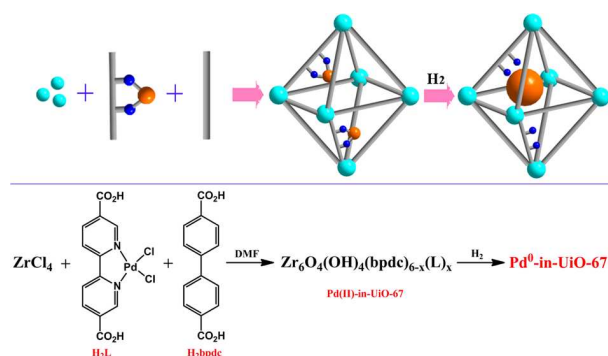
be removed from final MNPs–MOFs nanocomposites, which may have a negative impact on the catalytic properties of MNPs. The latter is the most widely utilised strategy, with a number of methodologies developed for the incorporation of NPs onto MOFs. These include chemical vapor deposition,¹³ solution infiltration,¹⁴ surface grafting,¹⁵ solid grinding,¹⁶ and microwave irradiation.¹⁷ These synthetic methods generally comprise two steps. In a first step, a metal precursor is firstly introduced into the porous network, followed by reduction of the embedded precursor in the second step to generate MNPs. For instance, Xu's group recently developed a double-solvent approach for the introduction of metal precursors within MOFs.¹⁸ Grzybowski *et al.* also demonstrated the use of a reductive MOF as matrix to generate metal NPs at the crystal core via a reaction-diffusion procedure.¹⁹ Despite increasing amount of work focusing on nanoparticle/MOF nanocomposites, the possibility to simply design advanced homogeneously distributed and controllable MNPs-embedded MOFs is a significant challenge which has not been addressed to date. Such difficulties come from the diffusion resistance between external and internal MOF surfaces, thus resulting in a random distribution of metal precursors on the MOF material. A general and facile method to simultaneously control the dispersed nature, spatial distribution, and confinement of incorporated nanoparticles within MOF matrices will offer the possibility to design advanced highly active and stable MNPs@MOFs catalytic materials.

Herein, we report, for the first time, the encapsulation of palladium precursors through ligand design prior to MOF assembling, which renders uniformly distributed palladium NPs inside the cavities of UiO-67. In contrast to previous reports, the proposed methodology can avoid the different diffusion resistance between external and internal surfaces, and thus allow metal precursors to be easily deposited into the pores and be evenly distributed through the MOF networks. In the course of the following reduction step, the anchoring sites on the ligands and the geometry of the MOF could synergistically restrict the growth of the metal NPs and fix them inside the pores. The as-prepared Pd-in-MOF composites exhibited excellent shape-selectivity in olefin hydrogenation, as well as high efficiency in aerobic oxidation of alcohols and reduction of nitrobenzene, showing significantly enhanced catalytic activities and stability as compared to those synthesized by a traditional impregnation method.

Results and discussion

A UiO-67 type MOF was chosen for this strategy due to high specific surface areas with an unprecedented stability present on UiO MOFs based on $Zr_6O_4(OH)_4(CO_2)_{12}$ secondary building units (SBUs) and dicarboxylate bridging ligands.²⁰ For the immobilization of Pd cations, 2,2-bipyride-5,5'-dicarboxylic acid was chosen as ligand due to the possibilities of 2,2-bipyride moieties to serve as anchor sites and their length matching well with that of biphenyldicarboxylic acid (H_2bpdcc , i.e., bridging ligand of UiO-67). The metalloligand H_2L was synthesized by treating $PdCl_2(CH_3CN)_2$ with dimethyl (2,2'-bipyridine)-5,5'-dicarboxylate, followed by base-catalyzed hydrolysis. A mixed ligand strategy was considered for the direct synthesis of Pd-UiO-67. Different Pd contents could be

loaded on UiO-67 by adjusting H_2L/H_2bpdcc ratios when assembling them into the MOF. The as-prepared Pd(II)-in-UiO-67 was treated under H_2 at 250 °C for 4 h to yield Pd⁰-in-UiO-67 (Scheme 2). For comparison, Pd was also loaded on the pre-synthesized UiO-67 by traditional impregnation method to yield Pd⁰/UiO-67.



Scheme 2. Synthesis of Pd⁰-in-UiO-67.

As measured by atomic absorption spectroscopy (AAS), we could achieve ca. 0.3, 0.6, 1.0, and 2.0 wt% Pd loadings, almost identical to those calculated from added starting materials to prepare the MOFs. However, only 0.6 wt % Pd was deposited for Pd⁰/UiO-67 prepared via traditional impregnation when a 2.0 wt % Pd loading was attempted. The majority of Pd was lost during the washing steps because most of such Pd precursor was loaded on the external surface of the MOF when using the impregnation method, easily removed by washing. Comparatively, the proposed strategy could facilitate the control of Pd loading on the MOF.

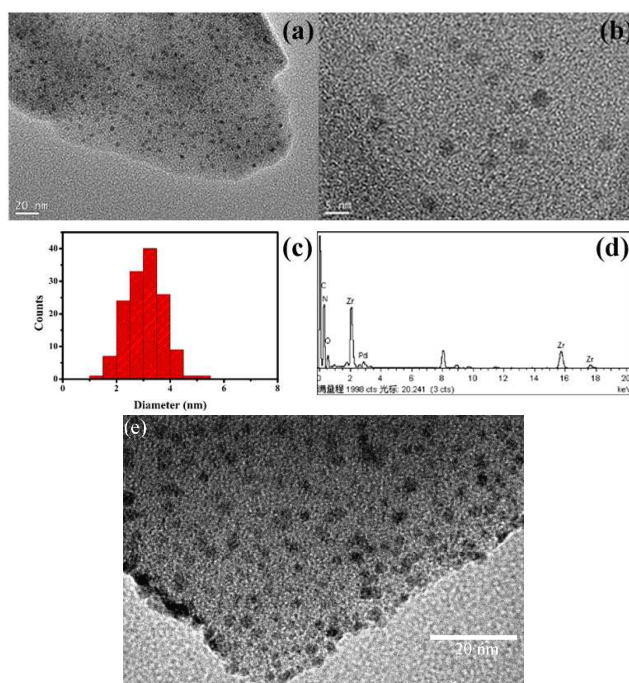


Figure 1. (a-b) TEM image of 1.0% Pd⁰-in-UiO-67, (c) corresponding size distribution of Pd nanoparticles, (d) EDX pattern and (e) TEM image of ultrathin cuts from 1.0% Pd-in-UiO-67.

Powder XRD patterns of the samples with different Pd loadings displayed no loss of crystallinity, suggesting that the integrity of the UiO-67 framework was well maintained after Pd modification (Fig. S1). The absence of a Pd diffraction pattern relates to the low Pd contents in the materials. Specific surface areas of the samples were measured by N₂ adsorption at 77 K, with results presented in Fig. S2 and Table S1. Nitrogen adsorption and surface areas of Pd⁰-in-UiO-67 samples were noticeably reduced as compared to pristine UiO-67, indicating that the cavities of UiO-67 may be occupied by highly dispersed Pd nanoparticles. At a same Pd loading, the nitrogen adsorption results of 0.6% Pd⁰/UiO-67 were significantly reduced with respect to those of 0.6% Pd⁰-in-UiO-67. These findings pointed to a potential pore blocking in Pd⁰/UiO-67 due to the incorporation of a large number of Pd NPs on the external surface of the MOF (thus restricting N₂ adsorption). As reported in the literature, the post-introduction of metal salts to a MOF network potentially leads to metal aggregation on the pore mouth, blocking the access to the internal surface.^{11a} The surface area of Pd⁰-in-UiO-67 was not drastically decreased, presumably due to that the Pd precursor was introduced through ligand design prior to MOF assembling. The Pd precursor could thus much easily enter the internal surface with the overcome diffusion resistance at the pore mouth. With this rational design, the aggregation of metal precursors on the pore mouth could be significantly restricted.

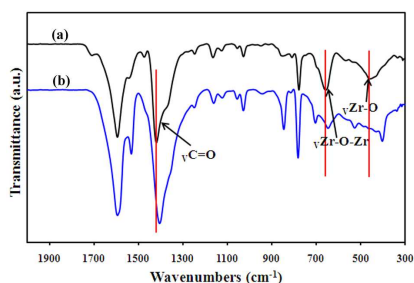


Figure 2. Infrared spectra of (a) UiO-67 and (b) 1.0% Pd-in-UiO-67.

TEM images of 1.0% Pd⁰-in-UiO-67 exhibited a uniform distribution of the Pd NPs in the UiO-67 framework with a mean size of 3.0 ± 0.5 nm (Figure 1). Only a slight aggregation was observed in the TEM images, indicating a high Pd dispersion. Only a small contribution of Pd particles could be observed bulging out from MOF edges (Figure 1e), suggesting that most Pd NPs were located inside UiO-67 (Figure 1e).

EDS analysis confirmed the presence of zero-valent Pd in Pd⁰-in-UiO-67. Note that particle sizes are somewhat exceeding the dimension of the MOF cavities (ca. 6.6 Å). Such a phenomenon might be attributed to local defects or deformations of the host framework as usually seen in other MNPs@MOFs composites.^{13b,15d} Because the loading level was quite low, these local defects did not significantly affect the overall structural integrity of the MOF. Comparably, TEM images of 1.0% Pd⁰/UiO-67 showed that Pd NPs, with a mean size of 5.5 ± 2.4 nm, were aggregated to some extent and many NPs were deposited on the external surface (Fig. S3).

Additionally, FT-IR spectra showed that UiO-67 could establish electron transfer to Pd NPs, evidencing the unique interaction

between MNPs and MOFs. The carbonyl, Zr-O-Zr, and Zr-O stretches at around 1425 cm⁻¹, 661 cm⁻¹, and 462 cm⁻¹ respectively, all displayed a slight red shift (Figure 2). This result indicates that the electron-rich carboxylate moiety of the secondary building unit in UiO-67 could donate electrons to the proximal palladium atoms, thus weakening both Zr-O and C=O bonds. Moreover, skeleton vibrations of benzene rings (at 1600-1500 cm⁻¹) were significantly disturbed, implying that aryl rings might also have electron donation effects to Pd NPs inside the cavities. The presence of such interactions observed from FT-IR spectra would support the conclusion that Pd NPs were uniformly distributed within the pores and had some chemical interactions with the MOF networks.

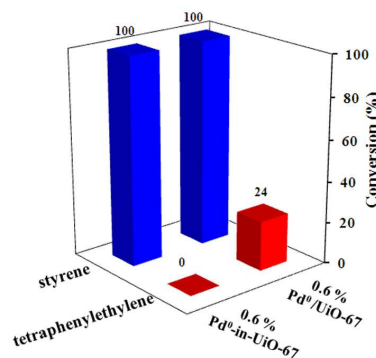


Figure 3. Comparison of 0.6% Pd-in-UiO-67 and 0.6% Pd⁰/UiO-67 in the hydrogenation of styrene and tetraphenylethylene. Reaction conditions: substrate (0.1 mmol), catalyst (Pd 1 mol%), THF (2 ml), 1 atm H₂, r.t., 1 h.

In order to further confirm that Pd NPs were indeed confined inside the cavities of UiO-67, 0.6% Pd⁰-in-UiO-67 was utilized as catalyst for the hydrogenation of two molecules (i.e., styrene and tetraphenylethylene) with different sizes. As a comparison, we also tested the catalytic activity of 0.6% Pd⁰/UiO-67 prepared via traditional impregnation method. As shown in Figure 3, both catalysts exhibited a high activity in styrene hydrogenation, providing identical conversions after 1 h. This indicated that there were no significant diffusional issues for UiO-67 framework because styrene was small enough (4.2 Å) to diffuse through the pore apertures. Importantly, the hydrogenation of a bulky substrate (tetraphenylethylene) provided remarkably different results for both samples. Pd⁰-in-UiO-67 gave no detectable activity, while Pd⁰/UiO-67 catalyst provided a comparably good activity. These findings demonstrated that Pd NPs deposited on the external surface of Pd⁰/UiO-67 played an important role in the hydrogenation reaction with respect to inaccessible encapsulated Pd NPs due to pore size limitations in Pd⁰-in-UiO-67 for molecules with a larger size such as tetraphenylethylene (6.7 Å). All results are consistent with TEM images.

The selective oxidation of alcohols is one of the most important transformations in organic chemistry.²¹ A range of supported transition-metal nanoparticles have been extensively utilized for these reactions.²² However, a large excess of base additives or expensive oxidizing agents have been employed in conjunction with harsh reaction conditions (e.g. high temperatures). In many cases, most catalysts can only be applicable to a very limited range of

substrates under base-free conditions. The development of a highly active and selective catalytic system which is more economical, environmentally benign, and easily recoverable is highly desirable.

The selective aerobic oxidation of cinnamyl alcohol was chosen as a model reaction to evaluate the activities of Pd-UiO-67 systems. Reactions were carried out under air atmosphere and base-free conditions. Parent UiO-67 showed no conversion of cinnamyl alcohol (Table 1, entry 1), confirming the requirement of a metal to perform the alcohol oxidation. The incorporation of Pd NPs significantly promoted the reaction. Results of the aerobic oxidation pointed to an optimized performance of 1.0% Pd⁰-in-UiO-67 (Table 1, entry 4), which provided quantitative conversion of cinnamyl alcohol to cinnamyl aldehyde at 80 °C within 20 h. The influence of solvent on the catalytic performance of the present reaction system was also investigated using 1.0% Pd⁰-in-UiO-67 catalyst, which indicated that toluene was the best solvent for this transformation under the investigated conditions (Table 1, entries 4, and 6–8).

Table 1. Results of the oxidation of cinnamyl alcohol.^a

Entry	Catalyst	Solvent	Conv. [%]	Sel. [%] ^b
1	UiO-67	Toluene	<1	99
2	0.3% Pd ⁰ -in-UiO-67	Toluene	73	>99
3	0.6% Pd ⁰ -in-UiO-67	Toluene	83	>99
4	1.0% Pd ⁰ -in-UiO-67	Toluene	>99	>99
5	2.0% Pd ⁰ -in-UiO-67	Toluene	>99	90
6	1.0% Pd ⁰ -in-UiO-67	DMF	11	>99
7	1.0% Pd ⁰ -in-UiO-67	CH ₃ CN	10	>99
8	1.0% Pd ⁰ -in-UiO-67	o-Xylene	95	>99
9 ^c	0.6% Pd ⁰ /UiO-67	Toluene	5	98
10 ^{c,d}	0.6% Pd ⁰ /UiO-67	Toluene	52	97
11 ^e	Reused 1.0% Pd ⁰ -in-UiO-67 (10 uses)	Toluene	99	>99
12	Pd/C	Toluene	51	72

^a Reaction condition: cinnamyl alcohol (1 mmol), catalyst (Pd 1 mol%), solvent (10 mL), 80 °C, 20 h, under air. ^b Yields were determined by GC-MS analysis. ^c 0.6% Pd⁰/UiO-67 was prepared by impregnation method. ^d 1 eq. NaOH was added. ^e Results of catalyst reused after ten cycles.

0.6% Pd⁰/UiO-67 was also tested under the same reaction conditions for comparative purposes. Only 5% conversion was obtained in 20 h (Table 1, entry 9). Interestingly, the yield was remarkably improved (50%, after 20 h reaction) when 1 eq. NaOH was added to the reaction mixture. The addition of base additives may promote the oxidation of alcohols by facilitating alcohol dehydrogenation steps. In comparison, 1.0% Pd⁰-in-UiO-67 exhibited much higher catalytic efficiency under identical conditions. This material features similar Pd loading and Pd mean particle size to 0.6% Pd⁰/UiO-67 (3.6 ± 1.0 nm, Fig. S4), (Table 1, entry 4). The superior efficiency of Pd⁰-in-UiO-67 in the oxidation of alcohol without the addition of bases may be due to the synergetic effects of nano-confinement and electron-donation of the UiO-67 framework. As Pd NPs were uniformly distributed in the pores of the MOF, the organic ligands would donate electrons to the Pd surfaces through coordination or π-bond interactions (as indicated by FT-IR spectra), which may facilitate the formation of anionic Pd. Such anionic Pd clusters are favorable for O₂ activation on Pd surfaces.²³ In contrast, abundant Pd NPs deposited on the external surface in Pd⁰/UiO-67 (as demonstrated by TEM analysis), have weak Pd-support electronic interactions as compared to Pd⁰-in-UiO-67, hence provide low or not

activity in the absence of bases. These findings support the previous supposition of the group related to the efficient oxidation conversion of alcohols by smaller Au NPs that was supposed to be confined in the cages of the MIL-101 support (although having no direct experimental proofs for the confinement).^{9a} For comparison, a 0.5% Pd/C catalyst was also tested in oxidation of cinnamyl alcohol under identical reaction conditions. 0.5%Pd/C possessed an almost identical particle size distribution to that of Pd⁰-in-UiO-67 (Fig. S5). Only 51% conversion with 72% selectivity to cinnamyl aldehyde was observed (Table 1, entry 12). These findings clearly support the speculation that nano-confinement and electron-donation effect offered by the MOF network could promote the selective oxidation of alcohols.

Table 2. Oxidation of various alcohols catalyzed by 1.0% Pd⁰-in-UiO-67.^a

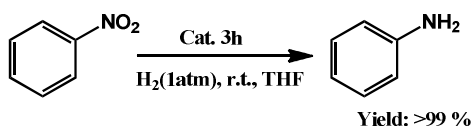
Entry	Substrate	Product	Time [h]	Yield [%] ^b
1			20	>99
2			15	>99
3			12	>99
4			40	98
5			20	99
6 ^c			20	>99
7 ^c			30	>99
8 ^d			30	96
9 ^d			30	98
10 ^d			20	98
11 ^d			20	97
12 ^d			20	98

^a Reaction condition: alcohol (1 mmol), 1.0% Pd⁰-in-UiO-67 (Pd 1 mol%), toluene (10 mL), 100 °C, under air. ^b Yields were determined by GC-MS analysis. ^c 80 °C. ^d Pd 2 mol%, 120 °C.

A variety of alcohols were then employed as substrates to investigate the scope of alcohols that can be tolerated in the aerobic oxidation under base-free and atmosphere air conditions using 1.0% Pd⁰-in-UiO-67 catalyst. The optimum catalyst was highly active and extremely selective for the oxidation of all substrates (Table 2). β-hydride elimination of a Pd-alcoholate species has been suggested to be the rate-determining step in the oxidation of alcohols to the corresponding carbonyl compounds.^{21b} Benzyl alcohols could be readily transformed to benzyl aldehydes (Table 2, entries 1-4), which are characterized by excellent selectivities and yields because of the conjugated effect of the aryl ring for the stabilization of the intermediate from the β-hydride elimination. Electronic variation on the aromatic substituents has some effects on the activity. Benzyl alcohols substituted with electron-donating groups such as CH₃, and OCH₃ (Table 2, entries 2 and 3) exhibited higher activity as compared to those with electron-withdrawing groups (entry 4).

Secondary benzylic alcohols were also converted to the corresponding ketones in quantitative yields (entry 5). The oxidation of allylic alcohols to their corresponding aldehydes is a facile reaction similar to the oxidation of benzyl alcohols.²¹ Allylic alcohols, for example, cinnamyl alcohol and trans-2-hexen-1-ol, were very active under the optimized condition, giving the desired products with high selectivities (entries 6 and 7). Aliphatic alcohols usually have a low reactivity in the documented alcohol oxidation. In particular, Pd⁰-in-UiO-67 was also a highly versatile advanced catalyst which could also be employed in the oxidation of aliphatic alcohols including linear and cyclic aliphatic alcohols, affording the corresponding ketones in 96-98% yields, although a higher Pd quantity (i.e., 2 mol% Pd) and temperature (i.e., 120 °C) were required (entries 8 and 9). This is most likely due to the stronger C_α-H bond strengths in aliphatic alcohols compared to those in benzylic and allylic alcohols.^{21b} Alcohols containing heteroatoms (e.g., nitrogen and sulfur), which are considered to strongly coordinate to metal active species,^{21c} could also be oxidized to the corresponding aldehyde compounds in excellent yields (entries 10-12) at high temperatures using higher Pd quantities.

The recyclability of the Pd⁰-in-UiO-67 catalyst was subsequently examined in the aerobic oxidation of cinnamyl alcohol. After the reaction, the catalyst was separated by centrifugation, thoroughly washed with toluene and then reused for a next reaction run under identical conditions with fresh reagents. The catalyst showed no appreciable reduction of activity even after ten runs (Table 1, entry 11). PXRD patterns for the reused catalyst suggested that the MOF matrix was completely preserved after several reuses (Fig. S1). TEM images revealed that Pd NPs were still well-dispersed in the reused catalyst, with an average diameter of 3.2 ± 0.5 nm (very similar to that of the as-synthesized sample, Fig. S6). These results indicated that no sintering of palladium NPs occurred during the reaction. The MOF framework should play an important role in preventing the encapsulated palladium NPs from aggregation during the reaction. The heterogeneous nature of the Pd⁰-in-UiO-67 was verified by hot filtration experiment at approximately 18% conversion, which showed that the isolated solution did not exhibit any further reactivity under similar reaction conditions. These findings were in good agreement with AAS experiments for which no Pd traces (below the detection limit) were detected in the reaction solution. Moreover, the Pd content of the reused catalyst was almost the same as the fresh one. These experiments indicated that the loss of palladium active sites was negligible and a heterogeneous oxidation reaction is taking place.



Scheme 3. Room temperature reduction of nitrobenzene for aniline formation.

Encouraged by these promising results, we further examined the catalytic activity of Pd⁰-in-UiO-67 in the reduction of nitrobenzene because of its importance in the industrial production of aniline.²⁴ Interestingly, Pd⁰-in-UiO-67 also exhibited a very high catalytic

activity in the hydrogenation of nitrobenzene (Scheme 3). Using 1.0% Pd⁰-in-UiO-67 as catalyst, nitrobenzene was fully reduced even under atmosphere pressure of H₂ and room temperature, leading to a quantitative yield of aniline in 3 h. It should be noted that our catalytic system represents a rare example for the quantitative hydrogenation of nitrobenzene under atmosphere pressure of H₂ and room temperature, which is comparable to the most active Pd supported catalysts ever reported²⁵ and comparably more efficient than reported MNPs catalysts supported on MOFs.²⁶

Conclusions

In summary, we have successfully developed, for the first time, a novel, facile and efficient strategy for the development of advanced Pd-MOF catalysts featuring encapsulated Pd NPs within the porous framework of UiO-67 via controllable introduction of metal precursors prior to MOF assembly. This strategy could also allow an accurate control of palladium loading onto MOFs. The confined Pd nanoparticles were highly active in the oxidation of alcohols and reduction of nitrobenzene, findings attributed to the electron donation and confinement effects offered by MOF networks, and thus exhibited significantly improved catalytic efficiencies compared with similar materials prepared by a traditional impregnation method. In addition, the catalyst was highly stable and reusable, without any particle aggregation/sintering after reaction. The achieved success in the encapsulation of metal NPs within MOF networks is envisaged to pave the way to new opportunities in the development of highly active and reusable heterogeneous catalysts for advanced catalysis applications (e.g. room temperature catalysis, aqueous processing).

Notes and references

^a School of Chemistry and Chemical Engineering, South China University of Technology, Guangzhou 510640 (China), E-mail: liyw@scut.edu.cn

^b Departamento de Química Orgánica, Universidad de Córdoba, Edif. Marie Curie, Ctra Nnal IV-A, Km 396, E14014, Córdoba (Spain), E-mail: q62alsor@uco.es

† Electronic Supplementary Information (ESI) available: [experimental details and catalysts characterization]. See DOI: 10.1039/c000000x/

- (a) L. Xu, W. Ma, L. Wang, C. Xu, H. Kuang, N. A. Kotov, *Chem. Soc. Rev.*, 2013, **42**, 3114; (b) H. Zhang, T. Watanabe, M. Okumura, M. Haruta, N. Toshima, *Nat. Mat.*, 2012, **11**, 49; (c) J. Lu, B. Fu, M. C. Kung, G. Xiao, J. W. Elam, H. H. Kung, P. C. Stair, *Science*, 2012, **335**, 1205.
- (a) B. R. Cuenya, *Acc. Chem. Res.*, 2013, **46**, 1682; (b) E. Gross, J. H. C. Liu, F. D. Toste, G. A. Somorjai, *Nat. Chem.*, 2012, **4**, 947; (c) G. Prieto, J. Zečević, H. Friedrich, K. P. de Jong, P. E. de Jongh, *Nat. Mat.*, 2013, **12**, 34; (d) I. Geukens, D. E. De Vos, *Langmuir*, 2013, **29**, 3170.
- (a) R. J. White, R. Luque, V. L. Budarin, J. H. Clark, D. J. Macquarrie, *Chem. Soc. Rev.*, 2009, **38**, 481; (b) X. Pan, Z. Fan, W. Chen, Y. Ding, H. Luo, X. Bao, *Nat. Mat.*, 2007, **6**, 507; (c) J. A. Farmer, C. T. Campbell, *Science*, 2010, **329**, 933.

- 4 (a) J. D. Evans, C. J. Sumby, C. J. Doonan, *Chem. Soc. Rev.*, 2014, DOI: 10.1039/C4CS00076E; (b) J. M. Campelo, D. Luna, R. Luque, J. M. Marinas, A. A. Romero, *ChemSusChem*, 2009, **2**, 18.
- 5 (a) H. Furukawa, K. E. Cordova, M. O’Keeffe, O. M. Yaghi, *Science*, 2013, **341**, 974; (b) W. Xuan, C. Zhu, Y. Liu, Y. Cui, *Chem. Soc. Rev.*, 2012, **41**, 1677; (c) H. Deng, S. Grunder, K. E. Cordova, C. Valente, H. Furukawa, M. Hmadeh, F. Gándara, A. C. Whalley, Z. Liu, S. Asahina, H. Kazumori, M. O’Keeffe, O. Terasaki, J. F. Stoddart, O. M. Yaghi, *Science*, 2012, **336**, 1018; (d) J. R. Li, J. Sculley, H. C. Zhou, *Chem. Rev.*, 2012, **112**, 869; (e) O. K. Farha, I. Eryazici, N. C. Jeong, B. G. Hauser, C. E. Wilmer, A. A. Sarjeant, R. Q. Snurr, S. T. Nguyen, A. O. Yazaydin, J. T. Hupp, *J. Am. Chem. Soc.*, 2012, **134**, 15016; (f) S. M. Cohen, *Chem. Rev.*, 2012, **112**, 970.
- 6 (a) J. Juan-Alcañiz, J. Gascon, F. Kapteijn, *J. Mater. Chem.*, 2012, **22**, 10102; (b) H. R. Moon, D. W. Limb, M. P. Suh, *Chem. Soc. Rev.*, 2013, **42**, 1807; (c) P. Valvekens, F. Vermoortele, D. De Vos, *Catal. Sci. Technol.*, 2013, **3**, 1435; (d) J. Hermannsdörfer, M. Friedrich, N. Miyajima, R. Q. Albuquerque, S. Kümmel, R. Kempe, *Angew. Chem. Int. Ed.*, 2012, **51**, 11473; (e) H. L. Jiang, T. Akita, T. Ishida, M. Haruta, Q. Xu, *J. Am. Chem. Soc.*, 2011, **133**, 1304.
- 7 A. Dhakshinamoorthy, M. Opanasenko, J. Čejka, H. Garcia, *Catal. Sci. Technol.*, 2013, **3**, 2509.
- 8 (a) J. Gascon, A. Corma, F. Kapteijn, F. X. Llabrés i Xamena, *ACS Catal.*, 2014, **4**, 361; (b) L. B. Vilhelmsen, K. S. Walton, D. S. Sholl, *J. Am. Chem. Soc.*, 2012, **134**, 12807; (c) L. B. Vilhelmsen, D. S. Sholl, *J. Phys. Chem. Lett.*, 2012, **3**, 3702.
- 9 (a) H. Liu, Y. Liu, Y. Li, Z. Tang, H. Jiang, *J. Phys. Chem. C*, 2010, **114**, 13362; (b) Y. K. Hwang, D. Y. Hong, J. S. Chang, S. H. Jung, Y. K. Seo, J. Kim, G. Férey, *Angew. Chem. Int. Ed.*, 2008, **47**, 4144; (c) Y. Huang, S. Liu, Z. Lin, W. Li, X. Li, R. Cao, *J. Catal.*, 2012, **292**, 111; (d) A. Dhakshinamoorthy, M. Alvaro, A. Corma, H. Garcia, *Dalton Trans.*, 2011, **40**, 6344; (e) Y. Zhao, J. Zhang, J. Song, J. Li, J. Liu, T. Wu, P. Zhang, B. Han, *Green Chem.*, 2011, **13**, 2078; (f) R. J. T. Houk, B. W. Jacobs, F. E. Gabaly, N. N. Chang, A. A. Talin, D. D. Graham, S. D. House, I. M. Robertson, M. D. Allendorf, *Nano Lett.*, 2009, **9**, 3413.
- 10 M. Ojeda, A. Pineda, A. A. Romero, V. Barron, R. Luque, *ChemSusChem*, 2014, DOI: 10.1002/cssc.201400055.
- 11 (a) A. Dhakshinamoorthy, H. Garcia, *Chem. Soc. Rev.*, 2012, **41**, 5262; (b) Y. Liu, Z. Tang, *Adv. Mater.* 2013, **25**, 5819; (c) M. Meilikhov, K. Yusenko, D. Esken, S. Turner, G. Van Tendeloo, R. A. Fischer, *Eur. J. Inorg. Chem.*, 2010, 3701.
- 12 (a) G. Lu, S. Z. Li, Z. Guo, O. K. Farha, B. G. Hauser, X. Y. Qi, Y. Wang, X. Wang, S. Y. Han, X. G. Liu, J. S. DuChene, H. Zhang, Q. C. Zhang, X. D. Chen, J. Ma, S. C. J. Loo, W. D. Wei, Y. H. Yang, J. T. Hupp, F. W. Huo, *Nat. Chem.*, 2012, **4**, 310; (b) Y. Liu, W. Zhang, S. Li, C. Cui, J. Wu, H. Chen, F. Huo, *Chem. Mater.*, 2014, **26**, 1119; (c) M. Zhang, Y. Yang, C. Li, Q. Liu, C. T. Williams, C. Liang, *Catal. Sci. Technol.*, 2014, **4**, 329; (d) T. Tsuruoka, H. Kawasaki, H. Nawafune, K. Akamatsu, *ACS Appl. Mater. Interfaces*, 2011, **3**, 378; (e) F. Ke, J. Zhu, L. G. Qiu, X. Jiang, *Chem. Commun.*, 2013, **49**, 1267; (f) P. Wang, J. Zhao, X. Li, Y. Yang, Q. Yang, C. Li, *Chem. Commun.*, 2013, **49**, 3330.
- 13 (a) S. Hermes, M. -K. Schröter, R. Schmid, L. Khodeir, M. Muhler, A. Tissler, R. A. Fischer, *Angew. Chem. Int. Ed.*, 2005, **44**, 6237; (b) D.-W. Lim, J. W. Yoon, K. Y. Ryu, M. P. Suh, *Angew. Chem. Int. Ed.*, 2012, **51**, 9814; (c) J. Hermannsdörfer, R. Kempe, *Chem. Eur. J.* 2011, **17**, 8071; (d) Y. K. Park, S. B. Choi, H. J. Nam, D.-Y. Jung, H. C. Ahn, K. Choi, H. Furukawa, J. Kim, *Chem. Commun.*, 2010, **46**, 3086.
- 14 (a) B. Yuan, Y. Pan, Y. W. Li, B. Yin, H. Jiang, *Angew. Chem. Int. Ed.*, 2010, **49**, 4054; (b) G. Chen, S. Wu, H. Liu, H. Jiang, Y. Li, *Green Chem.*, 2013, **15**, 230; (c) A. Aijaz, T. Akita, N. Tsumori, Q. Xu, *J. Am. Chem. Soc.*, 2013, **135**, 16356; (d) Y. E. Cheon, M. P. Suh, *Angew. Chem., Int. Ed.*, 2009, **48**, 2899; (e) C. Zlotea, R. Campesi, F. Cuevas, E. Leroy, P. Dibandjo, C. Volkringer, T. Loiseau, G. Férey, M. Latroche, *J. Am. Chem. Soc.*, 2010, **132**, 2991.
- 15 (a) Y. Pan, D. Ma, H. Liu, H. Wu, D. He, Y. Li, *J. Mater. Chem.*, 2012, **22**, 10834; (b) E. V. Ramos-Fernandez, C. Pieters, B. van der Linden, J. Juan-Alcañiz, P. Serra-Crespo, M. W. G. M. Verhoeven, H. Niemantsverdriet, J. Gascon, F. Kapteijn, *J. Catal.*, 2012, **289**, 42; (c) L. Shen, W. Wu, R. Liang, R. Lina, L. Wu, *Nanoscale*, 2013, **5**, 9374; (d) D. Esken, S. Turner, O. I. Lebedev, G. Van Tendeloo, R. A. Fischer, *Chem. Mater.*, 2010, **22**, 6393; (e) M. Martis, K. Mori, K. Fujiwara, W. S. Ahn, H. Yamashita, *J. Phys. Chem. C*, 2013, **117**, 22805.
- 16 (a) T. Ishida, M. Nagaoka, T. Akita and M. Haruta, *Chem. Eur. J.*, 2008, **14**, 8456; (b) H. L. Jiang, B. Liu, T. Akita, M. Haruta, H. Sakurai, Q. Xu, *J. Am. Chem. Soc.*, 2009, **131**, 11302.
- 17 M. S. El-Shall, V. Abdelsayed, A. E. R. S. Khder, H. M. A. Hassan, H. M. El-Kaderi and T. E. Reich, *J. Mater. Chem.*, 2009, **19**, 7625.
- 18 (a) A. Aijaz, A. Karkamkar, Y. J. Choi, N. Tsumori, E. Rönnebro, T. Autrey, H. Shioyama, Q. Xu, *J. Am. Chem. Soc.*, 2012, **134**, 13926; (b) Q. L. Zhu, J. Li, Q. Xu, *J. Am. Chem. Soc.*, 2013, **135**, 10210; (c) M. Yadav, Q. Xu, *Chem. Commun.*, 2013, **49**, 3327.
- 19 Y. Wei, S. Han, D. A. Walker, P. E. Fuller, B. A. Grzybowski, *Angew. Chem. Int. Ed.*, 2012, **51**, 7435.
- 20 J. H. Cavka, S. Jakobsen, U. Olsbye, N. Guillou, C. Lamberti, S. Bordiga, K. P. Lillerud, *J. Am. Chem. Soc.*, 2008, **130**, 13850.
- 21 (a) T. Mallat, A. Baiker, *Chem. Rev.*, 2004, **104**, 303; (b) K. Mori, T. Hara, T. Mizugaki, K. Ebitani, K. Kaneda, *J. Am. Chem. Soc.*, 2004, **126**, 10657; (c) Z. Hu, F. M. Kerton, *Appl. Catal. A-Gen.*, 2012, **413-414**, 332.
- 22 C. Parmeggiani, F. Cardona, *Green Chem.*, 2012, **14**, 547.
- 23 (a) A. Staykov, T. Kamachi, T. Ishihara, K. Yoshizawa, *J. Phys. Chem. C*, 2008, **112**, 19501; (b) A. V. Beletskaya, D. A. Pichugina, N. E. Kuz'menko, *Nanotechnologies in Russia*, 2011, **6**, 717.
- 24 G. Wienhöfer, I. Sorribes, A. Boddien, F. Westerhaus, K. Junge, H. Junge, R. Llusar, M. Beller, *J. Am. Chem. Soc.*, 2011, **133**, 12875.
- 25 (a) F. A. Harraz, S. E. El-Hout, H. M. Killa, I. A. Ibrahim, *J. Catal.*, 2012, **286**, 184; (b) D. Guin, B. Baruwati, S. V. Manorama, *Org. Lett.*, 2007, **9**, 1419; (c) S. Samanta, A. K. Nandi, *J. Phys. Chem. C*, 2009, **113**, 4721; (d) G. Kong, S. Ou, C. Zou, C. Wu, *J. Am. Chem. Soc.*, 2012, **134**, 19851.
- 26 W. Du, G. Chen, R. Nie, Y. Li, Z. Hou, *Catal. Commun.*, 2013, **41**, 56.